Available online at www.sciencedirect.com

ScienceDirect

Energy Procedia 55 (2014) 670 – 678

Energy Procedia

4th International Conference on Silicon Photovoltaics, SiliconPV 2014

Novel hybrid electrode using transparent conductive oxide and silver nanoparticle mesh for silicon solar cell applications

Mei Huang[a,*], Ziv Hameiri[a], Hua Gong[b], Wah-Chung Wong[b], Armin Gerhard Aberle[a], Thomas Mueller[a]

[a] *Solar Energy Research Institute of Singapore, National University of Singapore, 7 Engineering Drive 1, Block E3A, #06-01, Singapore 117574, Singapore*

[b] *Cima NanoTech, 1 Cleantech Loop, CleanTech One, #02-13, Singapore 637141, Singapore*

Abstract

Transparent conductive oxides (TCOs) have been widely used as the front electrodes for various solar cell structures, including heterojunction silicon wafer solar cells and the vast majority of thin-film solar cells. For heterojunction silicon wafer solar cells, the front TCO layer not only serves as a top electrode (by enhancing the lateral conductance of the underlying amorphous silicon film), but also as an antireflection coating. These requirements make it difficult to simultaneously achieve excellent conductivity and transparency, and thus only high-quality indium tin oxide (ITO) has as yet found its way into industrial heterojunction silicon wafer solar cells. For thin-film solar cells, in order to provide efficient lateral conductance of the charge carriers, normally a TCO layer of a few hundred nanometers thickness is used which impedes the optical transparency due to the enhanced free carrier absorption. To reduce the conflict between conductivity and transparency, and to separately engineer the electrical and optical properties, a hybrid electrode is proposed and fabricated by us which consists of a TCO layer (optical layer) and a silver nanoparticle mesh (electrical layer). This hybrid electrode is demonstrated to have a 10 times higher lateral conductance compared to a single TCO layer, while maintaining high light transmission in a wide wavelength range. Due to the excellent performance of the hybrid electrode, it is demonstrated that such an electrode is suitable for various solar cell structures.

Peer-review under responsibility of the scientific committee of the SiliconPV 2014 conference

Keywords: heterojunction; thin film; transparent conductive oxides; silver nanoparticles; solar cells

* Corresponding author. Tel.: +65 86441246; fax: +65 67751943.
E-mail address: huang.mei@nus.edu.sg

Peer-review under responsibility of the scientific committee of the SiliconPV 2014 conference
doi:10.1016/j.egypro.2014.08.043

1. Introduction

Transparent conductive oxides (TCOs) are widely used as the front electrode for a variety of solar cell structures. The ideal TCOs to be used as the front electrode should be fully transparent in a wide wavelength range and have metal-like conduction properties; however this is not the case for real TCO materials. Due to the limited conductivity and non-negligible light absorption of TCOs, there is always a trade-off between conductivity and transparency. For heterojunction (HET) silicon wafer solar cells, which feature an amorphous silicon layer stack on the illuminated surface, the use of TCO is not only for lateral carrier transport, but also to provide good antireflection properties. These requirements constrain the carrier concentration and thickness of the TCO, thus making it a challenge to optimize both the electrical and the optical performances. Indium tin oxide (ITO) is the most commonly used TCO material for HET solar cells, due to its excellent electrical and optical properties. Current deposition techniques are able to form ITO films with resistivities in the range of 10^{-5} to 10^{-4} Ωcm while maintaining the optical transmissions in the range of 80-90 % [1-6]. Due to the high cost of ITO, there is increasing interest in more cost-effective materials such as aluminum-doped zinc oxide (AZO) and gallium-doped zinc oxide (GZO). However, the efficiencies of HET solar cells using the cost-effective materials are lower due to the increased resistive losses in the TCO layer [7, 8]. For thin-film solar cells, due to the poor lateral conductance of the thin active layer, a thicker TCO layer of up to 1 μm thickness is normally used which results in low light transmission in the long wavelength range due to the increased free carrier absorption.

One possibility to reduce the sheet resistance of the front electrode is to add a more conductive layer in between of two TCO layers, for example a thin metal layer, to form a multilayer structure [9, 10]. Although the lateral conductance of such structures is greatly enhanced, the overall transmission suffers for large parts of the solar spectrum, making this approach unsuitable for solar cell applications. Another alternative approach is to use the metal mesh networks that are fabricated using either patterning methods or wet-coating processes of nanostructures (i.e. nanoparticles, nanowires). Commonly used patterning methods include lithography [11, 12] and direct writing methods by inkjet printing [13, 14]. The patterning methods are able to form regular and periodic structures, with an accurate control of the network line width down to the nanoscale range; however they are limited to small-area devices due to the complex and time-consuming fabrication processes. The wet-coating methods, including spin coating [15], Meyer rod coating [16] and spray coating [17] are normally solution based. Therefore, they are easier and cheaper to be applied to large-area devices such as solar cells. Given the fact that the optimal sheet resistance of the front electrode used in a solar cell should be below 10 Ω/□ [18], only a few highly transparent materials with comparable sheet resistance are suitable for photovoltaic applications.

In order to enhance the lateral conductance of the front electrode, a silver nanoparticle mesh is used in this study as an electrical layer which exhibits a sheet resistance below 5 Ω/□ and 90 % transparency in the visible range (380-780 nm) of the spectrum. In this work, two hybrid structures (A and B) that are fabricated by superimposing the silver nanoparticle mesh with a TCO layer are proposed for different applications. Hybrid structure A (see Fig. 3a) targets applications in HET silicon wafer solar cells (or substrate thin-film solar cells, e.g. CIGS solar cells). It uses an 80 nm thick TCO layer as an antireflection coating onto which a silver nanoparticle mesh is deposited. This structure allows to separately engineer the electrical and optical properties of the front electrode: the electrical layer (i.e. the silver mesh) provides sufficient lateral conductance for the charge carriers while the optical layer (i.e. the TCO layer) mainly functions as an antireflection coating (but also provides a short-distance lateral conduction path towards the silver mesh) [19]. Hybrid structure B (see Fig. 3b) is not very different from the hybrid structure A. It aims for applications in superstrate thin-film solar cells (e.g. organic solar cells, amorphous silicon solar cells, CdTe solar cells, etc.). The silver nanoparticle mesh is inserted between the glass substrate and the solar cell structure, which forms a hybrid electrode with the TCO layer. Due to the good lateral conductance of the silver mesh, the lateral conductance of a thin TCO layer (around 100 nm) is sufficient for carrier conduction in between of the silver lines. For both structures, cost-effective TCO materials, such as AZO, can be used to further reduce the device cost.

2. Silver nanoparticles

The silver nanoparticles (proprietary SANTE® technology, Cima NanoTech) are initially embedded and suspended in a solvent emulsion. After a wet-coating process at atmospheric pressure, the nanoparticles self-assemble into a random mesh-like network on the coated substrate due to the evaporation of the solvents. The formed network is composed of closely packed nanoparticles (bonded with resin contained in the emulsion). After either a thermal or chemical (hydrochloric acid dip) post-coating treatment, the silver nanoparticle mesh becomes highly conductive. Excluding the mesh network covered region, the openings between the silver lines are 100 % transparent (and non-conductive). Advantages of this approach include: (i) mask-less coating process, and (ii) inexpensive deposition tool. These features ensure a simple and low-cost process. Furthermore, the formed silver mesh is compatible with a large-area roll-to-roll process, which is easy to be adapted for mass production.

Scanning electron microscope (SEM) micrographs of the silver nanoparticle mesh and the morphology of the silver nanoparticles on a PET substrate are shown in Fig. 1. The height of the silver nanoparticle lines is in the range of 3 μm, while the average 'pore' size in this study is around 200 μm. The pore size is variable, by adjusting the silver emulsion accordingly. The diameter of the silver nanoparticles is about 50 nm. The area coverage of the silver mesh is about 12 % (we determined an average value of 11.8 % on 10 different samples via image processing, by extracting the shading percentage within a certain color threshold).

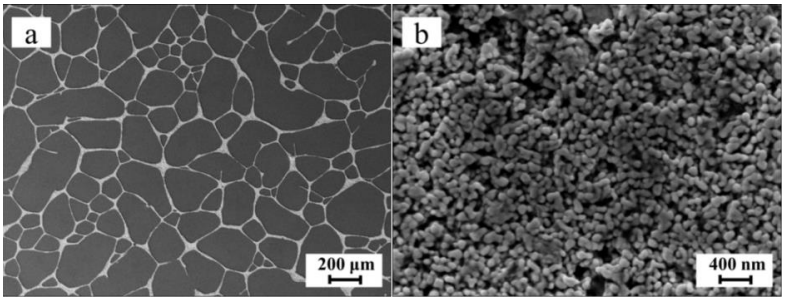

Fig. 1. SEM images of the silver nanoparticle mesh: (a) pattern on PET substrate, (b) morphology of silver nanoparticles.

3. Experiment

For characterization purposes, clear quartz glass plates of 125 mm × 125 mm size were used as substrates. The substrates were cleaned in an ultrasonic bath using isopropyl alcohol (IPA) and acetone, followed by a deionized (DI) water rinse. The substrates were then dried in a nitrogen environment at 80 ºC for 30 minutes. Two types of TCO - ITO and AZO - were used in this study. Both were deposited by radio frequency (RF) magnetron sputtering at 5 mTorr and 150 °C, using ceramic targets.

For hybrid structure A the silver nanoparticle mesh is directly coated on the TCO. However, due to the low wettability of TCO surfaces, the direct coating of the silver nanoparticle mesh onto TCO-coated substrates is still a challenge at this stage. This issue can be tackled in future work, for example by the use of an oxygen plasma [20] or an ultraviolet (UV) ozone treatment [21]. Currently, the transfer technique is employed by us as a temporary measure for testing purposes. The silver nanoparticle mesh is transferred from a PET product (donor, SANTE FS110, Cima NanoTech) to the TCO coated substrate (receiver), using a UV curing resin (see below for more details). The transfer method is capable to form the silver mesh structure on various substrates, without modification of the emulsion. Besides being suitable for glass based devices, the transfer method is a useful tool to examine the performance of the hybrid structure before its application to a solar cell structure.

For most of the thin-film devices, due to the fact that the total thickness of the p-i-n structure is normally less than a few micrometers, a high surface roughness appearing over a small area may create shunting, which degrades the device's PV performance [22]. Since the silver nanoparticle mesh covered region is 3 μm in height, it is

detrimental to be applied directly onto superstrate thin-film solar cell devices. By using the transfer method, the silver mesh is fully embedded in the resin which helps to eliminate sharp features on the surface, therefore effectively avoiding the shunting problem. Due to the fact that the openings between the silver lines are not conductive, a thin TCO layer is needed to assist the carrier conduction; however, the TCO layer doesn't need to be so conductive, as the charge carriers do not have to travel a long distance to reach the silver mesh.

The transfer steps are illustrated in Fig. 2. First, a thin layer of UV-curing resin is coated onto the substrate by a Meyer rod [Fig. 2(a)]. Next, the donor PET foil coated with a silver nanoparticle mesh is attached to the resin wetted substrate and the sample is then loaded into a laminator operating at 80 ºC at a speed of 5 mm/s [Fig. 2(b)]. This process fully embeds the silver mesh in the resin. In the next step, the laminated stack is loaded into a UV system. The UV system is employed to activate and harden the resin at 0.212 J/cm^2 UV light intensity and conveyer speed of 3 cm/s [Fig. 2(c)]. After the hardening process is completed, the PET substrate can be easily (and fully) peeled off, leaving the silver nanoparticle mesh on the substrate [Fig. 2(d)]. The final hybrid structures targeted for different solar cells structures are shown in Fig. 3.

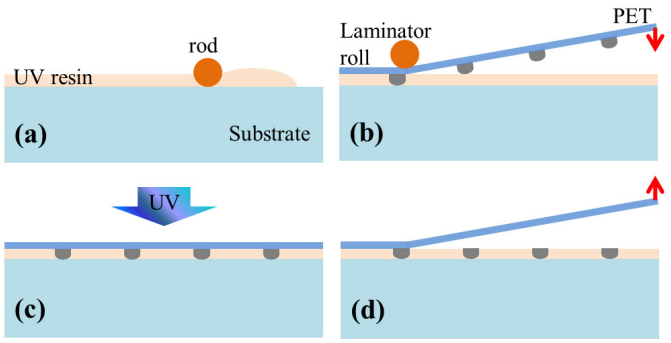

Fig. 2. Transfer procedure of the silver nanoparticle mesh to a target substrate: (a) UV resin coating using a Meyer rod; (b) laminating the stack in a hot laminator; (c) hardening of the resin using UV exposure; (d) peel off PET substrate to finish the transfer.

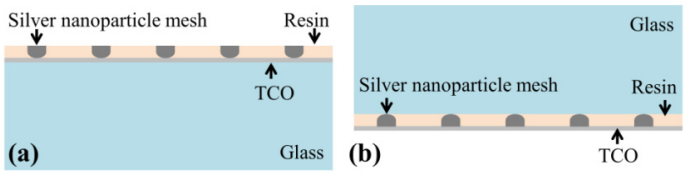

Fig. 3. Final hybrid structures on glass substrate for different solar cell structures: (a) HET silicon wafer solar cell; (b) superstrate thin-film solar cells.

For the following study, two reference samples were prepared: a sample with a 20 nm thick TCO film covered on half of its surface by the silver nanoparticle mesh was fabricated to test the contact conditions between the TCO and the silver mesh; furthermore, a bare glass pane with only a cured resin layer (of the same thickness as that used in the hybrid structure) was prepared as a reference sample to estimate the transmission of the hybrid structure without the influence of the resin. Four samples were prepared for the investigation of hybrid structure A: Two groups of 80 nm TCO samples, one with and the other without the silver mesh, were used to compare the electrical and optical performance of the standard structure (TCO only) and the hybrid structure. The other five TCO samples, three samples with only TCO layer and two samples with the hybrid structure of different ITO thicknesses, were prepared for the study of hybrid structure B. Details of the samples are listed in Table 1.

Table 1. Vertical structure of the prepared samples on top of glass substrate.

Reference samples			Vertical structure of hybrid structure A			Vertical structure of hybrid structure B		
Sample	Substrate coating	Silver mesh	Sample	Substrate coating	Silver mesh	Sample	Silver mesh	Surface coating
1	Resin	No	1	80 nm ITO	No	1	No	60 nm ITO
2	20 nm ITO	Yes (half area)	2	80 nm ITO	Yes	2	Yes	60 nm ITO
			3	80 nm AZO	No	3	No	120 nm ITO
			4	80 nm AZO	Yes	4	Yes	120 nm ITO
						5	No	1 μm AZO

The sheet resistance was determined by a four-point probe (Loresta-GP MCP-T610 with ESP-type probes, Mitsubishi). The spectral dependence of the transmission was measured by a UV/Vis/NIR spectrophotometer (Lambda 1050, PerkinElmer), while the transmission at visible wavelengths (380-780 nm) [23] was obtained by a haze meter (NDH 5000, Nippon). The sample surface morphology and the cross-section were investigated with an SEM (Auriga, Zeiss).

4. Results and discussions

4.1. Hybrid structure A

The interfacial and cross-section SEM images of the hybrid structure A are illustrated in Fig. 4. Figure 4(a) shows a top-view SEM image of the interfacial region of the silver nanoparticles and the UV-treated resin. The cross-sectional image of the hybrid structure in Fig. 4(b) shows that physical contacts between the silver line and the TCO film have been established.

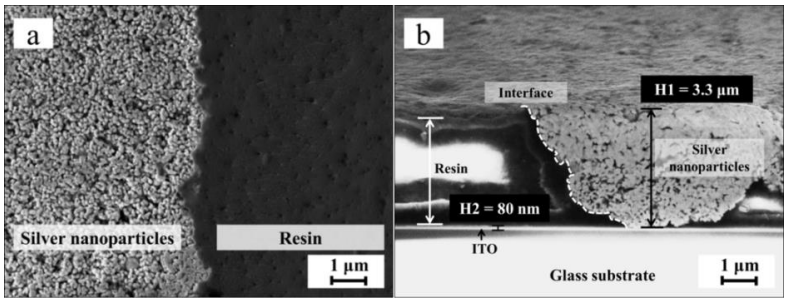

Fig. 4. SEM images of the ITO/silver nanoparticle mesh hybrid structure: (a) top-view of the interface between the silver nanoparticles and the resin; (b) cross-sectional view of the silver mesh on top of an 80 nm ITO layer.

The electrical contact between the ITO layer and the silver nanoparticle mesh was examined on the reference sample 2 by using an ohmmeter (equipped with two 2 mm diameter probes). Whenever the two probes were in contact with the ITO and the silver mesh, a quantifiable resistance was obtained, indicating that electrical contacts between the ITO and the silver mesh were established. The sheet resistance and the average visible transmission of different samples are listed in Table 2. A large reduction of the sheet resistance, by more than a factor of 10, was observed after transferring the silver mesh onto the TCO-coated glass substrate. It is noted that this large reduction was accomplished with only a moderate reduction of the visible transmission. We suspect that some forward scattering occurs due to the localized surface plasmonic resonance of the silver nanoparticles, which compensates some of the shading loss. Of particular interest is the hybrid structure involving AZO. This structure demonstrates almost identical properties as that made with the more expensive ITO film. The corrected visible transmission, representing the transmission of the transparent conductive layer/layer stack excluding the influence of the substrate,

is calculated by dividing the transmission of the sample by that of the bare glass plate ($T_{visible}$: 92.4 %). The figure-of-merit of the transparent conductors (Φ_{TC}) is calculated based on the following equation [24]:

$$\Phi_{TC} = \frac{T^{10}}{R_s}, \quad (1)$$

where here the T is the corrected average transmission in the visible range and R_s is the sheet resistance of the structure to be quantified.

Table 2. Sheet resistance and visible transmission of TCO single layers and hybrid structures.

Properties	80 nm ITO		80 nm AZO	
	As coated	Hybrid structure	As coated	Hybrid structure
R_s (Ω/□)	47±1.2	4.7±0.2	180±5.0	4.8±0.3
$T_{visible}$ (%)	82.5±0.1	79.5±0.2	84.5±0.1	79.6±0.2
$T_{corrected\ visible}$ (%)	89.3	86.0	91.5	86.1
Φ_{TC} (Ω^{-1})	6.68×10^{-3}	4.71×10^{-2}	2.29×10^{-3}	4.66×10^{-2}

Figure 5 compares the optical transmission (bare glass as reference in UV/Vis/NIR measurement) of the ITO hybrid structure with that of a standard sample having an 80 nm thick ITO film. As can be seen, even with the influence of the resin, the hybrid structure maintains a high transmission of well above 80 % in the 400 to 1500 nm wavelength range. The reduced transmission is due to the shading loss from the silver mesh network and the additional transmission loss caused by the resin layer. The estimated transmission after elimination of the loss caused by the resin layer (by using a resin coated glass as a reference sample in UV/Vis/NIR measurement, $T_{visible}$ = 90.4 %) predicts that once the direct coating of the silver nanoparticle mesh is realised, the hybrid structure will have a transmission of above 85 % over the wavelength range from 400 to 1500 nm.

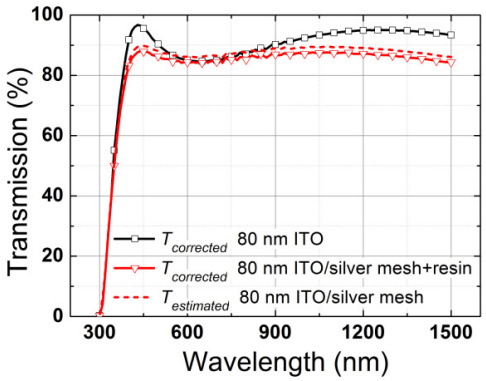

Fig. 5. Optical transmission as a function of wavelength of a hybrid ITO/silver nanoparticle mesh sample (red solid line with triangles) and a standard sample with 80 nm ITO thickness (black line with squares). Also shown (red dashed line) is the estimated optical transmission of the hybrid structure after elimination of the influence of the resin layer.

4.2. Hybrid structure B

Hybrid structure B is designed for superstrate thin-film solar cells which include the glass substrate as part of the solar cell structure. The electrical and optical performances of the hybrid structure B are listed in Table 3. As the TCO layer of this hybrid structure is not fixed to a certain thickness as a optical functional layer, using the visible transmission is not a suitable parameter. Instead, the weighted average transmission (WAT) of the glass sample

(including the influence of the glass substrate) is applied:

$$\mathrm{WAT}_{300\mathrm{nm},\ 1200\mathrm{nm}} = \frac{\sum_i T(\lambda_i) N_{\mathrm{AM1.5}}(\lambda_i)}{\sum_i N_{\mathrm{AM1.5}}(\lambda_i)}\ , \tag{2}$$

where $T(\lambda_i)$ is the wavelength dependent transmission and $N_{\mathrm{AM1.5}}$ is the photon flux of the incident solar radiation (given in $m^{-2}\ s^{-1}\ nm^{-1}$).

The figure of merit is calculated based on the above WAT value by replacing the T in Eq. 1. Compared to a single TCO layer, the corresponding hybrid structures reveal better lateral conductance, as shown in Table 3. However, it is also found that the total transmissions for both 60 nm and 120 nm ITO hybrid structure are reduced by approximately 10 % compared to the single TCO layer. This large reduction is due to the shading loss caused by the silver mesh, the additional absorption losses in the resin layer, and the losses due to the non-optimized TCO coating (which all can be further reduced in future work). For example, as the silver mesh is two times more conductive than the required sheet resistance of the front electrode, it can be optimized by adjusting the coating emulsion to have larger pore size, so as to reduce the shading loss. Since the sheet resistance of the hybrid structure is approximately the parallel resistance of the composing layers, it follows that the contact resistance between the silver nanoparticle mesh and the TCO layer is negligible. By using a relatively more resistive and more transparent TCO layer, the sheet resistance of the hybrid structure is smaller than that of the silver mesh, while the overall transmission of the hybrid structure is improved.

Table 3. Sheet resistance and weighted average transmission of TCO single layers and hybrid structures.

Properties	60 nm ITO		120 nm ITO		1 μm AZO
	As coated	Hybrid structure	As coated	Hybrid structure	As coated
R_s (Ω/□)	76±1.0	4.4±0.1	38±0.6	4.2±0.1	7.5±0.5
WAT (%)	80.0	69.2	80.6	69.8	76.4
Φ_{TC} (Ω^{-1})	1.41×10^{-3}	5.72×10^{-3}	3.04×10^{-3}	6.53×10^{-3}	9.03×10^{-3}

The optical transmission curves of different transparent conductive structures are shown in Fig. 6. The hybrid structures with either 60 nm or 120 nm ITO coating are shown to have improved transmission at short wavelengths (near the light absorption edge). As only a thin TCO layer is used in the presented hybrid structure, the free carrier absorption associated with light transmission in the long wavelength range is reduced consequently as compared to the 1 μm thick AZO layer.

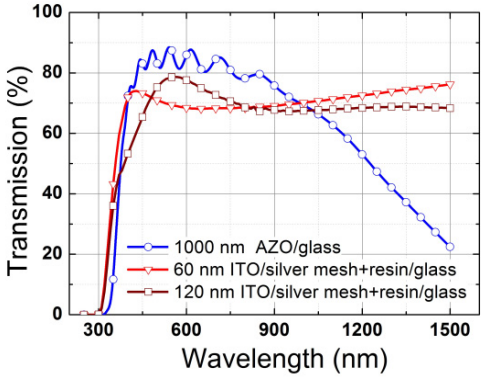

Fig. 6. Optical transmission of the hybrid structure B with 60 nm and 120 nm ITO coating on glass substrates. Also shown is the optical transmission of the 1 μm thick AZO film.

4.3. Adhesion test

Adhesion test for both hybrid structures was done by using the crosshatch testing method (cross-cut tester, BYK-Gardner) [25]. As shown in Fig. 7, the hybrid samples were cut with a blade into of 1 mm wide squares all the way to the glass substrate, to form a 90° lattice pattern. The tested region was then brushed five times in a diagonal direction before adhesion test using a sticky tape (Intertape Polymer 51596). The smooth edges around the cutting region and the fact that none of the squares was detached after tape test, indicates a good adhesion between the transferred mesh and the underlying TCO layer.

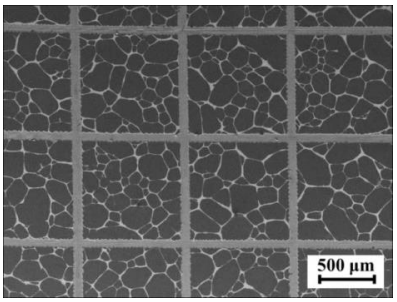

Fig. 7. Top-view SEM image of the ITO hybrid structure after an adhesion test.

5. Conclusion

Owing to the good electrical properties of the silver mesh, which are superior to those of silver nanowire and nanoparticle meshes reported previously [12, 15], the lateral conductance of the hybrid structures is greatly reduced by one order of magnitude, with only a moderate reduction in the optical transmission. Our hybrid structure also has a higher lateral conductance and transparency than the hybrid structures formed by silver nanowires (using either carbon nanotubes [26] or titanium dioxide [27]). The obtained transmission is similar to that of grid patterns formed by silver nanoparticles with a 200 µm pitch [13]. Note that these superior results were obtained by a process which is much simpler and cheaper than those previously used. Since the silver nanoparticle mesh can be formed via a wet-chemical coating process, it is possible to create patterns with different opening sizes and line widths in order to optimize the optical and electrical performances. It is believed that these hybrid structures can be easily applied to several solar cell structures. Future work will focus on direct formation of the silver mesh on the TCO surface, thereby eliminating the loss associated with the resin used in the present process.

Acknowledgements

The Solar Energy Research Institute of Singapore is supported by the National University of Singapore (NUS) and Singapore's National Research Foundation (NRF) through the Singapore Economic Development Board (EDB). This research was sponsored by NRF grant NRF2010EWT-CERP001-022. The support of Cima NanoTech Singapore is acknowledged. The authors would like to thank Mr Yan Xia for providing the transmission data of the AZO film (Fig. 6).

References

[1] Das R, Adhikary K, Ray S. The role of oxygen and hydrogen partial pressures on structural and optical properties of ITO films deposited by reactive rf-magnetron sputtering. Appl. Surf. Sci. 2007; **253**:6068-73.

[2] Guillén C, Herrero J. Influence of oxygen in the deposition and annealing atmosphere on the characteristics of ITO thin films prepared by sputtering at room temperature. Vacuum 2006; **80**:615-20.

[3] Kerkache L, Layadi A, Dogheche E, Rémiens D. Annealing effect in DC and RF sputtered ITO thin films. Eur. Phys. J. Appl. Phys. 2007; **39**:1-5.
[4] Lippens P, Büchel M, Chiu D, Szepesi C. Indium–tin-oxide coatings for applications in photovoltaics and displays deposited using rotary ceramic targets: Recent insights regarding process stability and doping level. Thin Solid Films 2013; **532**:94-97.
[5] Manavizadeh N, Boroumand FA, Asl-Soleimani E, Raissi F, Bagherzadeh S, Khodayari A, Rasouli MA. Influence of substrates on the structural and morphological properties of RF sputtered ITO thin films for photovoltaic application. Thin Solid Films 2009; **517**:2324-27.
[6] Holman ZC, Filipič M, Descoeudres A, De Wolf S, Smole F, Topič M, Ballif C. Infrared light management in high-efficiency silicon heterojunction and rear-passivated solar cells. J. Appl. Phys. 2013; **113**:013107.
[7] Schüttauf JA. Amorphous and crystalline silicon based heterojunction solar cells. PhD thesis, Utrecht University, 2011.
[8] Choong G, Bôle P, Barraud L, Zicarelli Fernandez F, Descoeudres A, De Wolf S, Ballif C. Transparent conductive oxides for silicon heterojunction solar cells. Proc. 25th EU PVSEC 2010; pp. 2505-10.
[9] Guillén C, Herrero J. Transparent conductive ITO/Ag/ITO multilayer electrodes deposited by sputtering at room temperature. Opt. Commun. 2009; **282**:574-78.
[10]Sahu DR, Huang J-L. High quality transparent conductive ZnO/Ag/ZnO multilayer films deposited at room temperature. Thin Solid Films 2006; **515**:876-79.
[11]van de Groep J, Spinelli P, Polman A. Transparent conducting silver nanowire networks. Nano Lett. 2012; **12**:3138-44.
[12]Layani M, Magdassi S. Flexible transparent conductive coatings by combining self-assembly with sintering of silver nanoparticles performed at room temperature. J. Mater. Chem. 2011; **21**:15378-82.
[13]Ahn BY, Lorang DJ, Lewis JA. Transparent conductive grids via direct writing of silver nanoparticle inks. Nanoscale 2011; **3**:2700-02.
[14]Layani M, Gruchko M, Milo O, Balberg I, Azulay D, Magdassi S. Transparent conductive coatings by printing coffee ring arrays obtained at room temperature. ACS Nano 2009; **3**:3537-42.
[15]Xie S, Ouyang Z, Jia B, Gu M. Large-size, high-uniformity, random silver nanowire networks as transparent electrodes for crystalline silicon wafer solar cells. Opt. Express 2013; **21**:A355-62.
[16]Liu CH, Yu X. Silver nanowire-based transparent, flexible, and conductive thin film. Nanoscale Res. Lett. 2011; **6**:75.
[17]Scardaci V, Coull R, Lyons PE, Rickard D, Coleman JN. Spray deposition of highly transparent, low-resistance networks of silver nanowires over large areas. Small 2011; **7**:2621-28.
[18]Hecht DS, Hu L, Irvin G. Emerging transparent electrodes based on thin films of carbon nanotubes, graphene, and metallic nanostructures. Adv. Mater. 2011; **23**:1482-513.
[19]Huang M, Hameiri Z, Gong H, Wong W-C, Aberle AG, Mueller T. Hybrid silver nanoparticle and transparent conductive oxide structure for silicon solar cell applications. Phys. Status Solidi - Rapid Res. Lett. 2014; **8**:399-403.
[20]Tang F-C, Chang J, Chou W-Y., Cheng H-L, Hsu S. L-C, Chen J-S, Sheu H-S. Effective oxygen plasma treatment on indium tin oxide electrode to improve organic solar cell efficiency. Phys. Status Solidi A 2012; **209**:369-72.
[21]Li CN, Djurišić AB, Kwong CY, Lai PT, Chan WK, Liu SY. Indium tin oxide surface treatments for improvement of organic light-emitting diode performance. Appl Phys A 2005; **80**:301-07.
[22]Galagan Y, Andriessen R. Organic Photovoltaics: Technologies and Manufacturing. Third Generation Photovoltaics, 2012.
[23]D1003. ASTM International standard test method for haze and luminous transmittance of transparent plastics, West Conshoocken, PA.
[24]Haacke G. New figure of merit for transparent conductors. J. Appl. Phys. 1976; **47**:4086-89.
[25]D3359. ASTM International standard test methods for measuring adhesion by tape test, West Conshoocken, PA.
[26]Tokuno T, Nogi M, Jiu J, Suganuma K. Hybrid transparent electrodes of silver nanowires and carbon nanotubes: a low-temperature solution process. Nanoscale Res. Lett. 2012; **7**:281.
[27]Zhu R, Chung C-H, Cha KC, Yang W, Zheng YB, Zhou H, Song T-B, Chen C-C, Weiss PS, Li G, Yang Y. Fused silver nanowires with metal oxide nanoparticles and organic polymers for highly transparent conductors. ACS Nano 2011; **5**:9877-82.